The Flinders University of South Australia

ELECTRONIC STRUCTURE OF MATERIALS CENTRE

Convergent Close-Coupling Calculations of Electron-Helium Scattering

Dmitry V. Fursa and Igor Bray

Submitted to J. Phys. B as a Topical Review

ESM-143

November 1996

TOPICAL REVIEW

Convergent close-coupling calculations of electron-helium scattering

Dmitry V. Fursa and Igor Bray †,

Electronic Structure of Materials Centre, The Flinders University of South Australia, G.P.O. Box 2100, Adelaide 5001, Australia

Abstract. We present a review of the recent electron-helium calculations and experiments concentrating on the extensive application of the convergent close-coupling (CCC) method. Elastic, excitation, and ionization processes are considered, as well as excitation of the metastable states. The present status of agreement between theory and experiment for elastic and discrete excitations of the ground state is, in our view, quite satisfactory. However, discrepancies for excitation of the metastable states are substantial and invite urgent attention. Application of the CCC method to the calculation of differential ionization cross sections is encouraging, but also shows some fundamental difficulties.

PACS numbers: 34.80.Bm,34.80.Dp

Short title: TOPICAL REVIEW

Submitted to: J. Phys. B: At. Mol. Opt. Phys.

October 17, 1996

† e-mail: I.Bray@flinders.edu.au

1. Introduction

Electron-helium scattering is the second most simplest electron-atom scattering system only being surpassed by the electron-hydrogen problem. The former has substantial advantages from the experimental point of view and has been used as a standard against which other scattering systems may be compared, normalised, calibrated, etc. For theorists the e-H system is preferable primarily because a three-body system is easier to work with than a four-body system. For these reasons over the years there has been a disproportional concentration of theoretical and experimental activity: a great deal of e-H theory with relatively little experimental support and vice versa for the e-He system.

It turned out that the theorist's fear, at least our own, of the e-He problem was somewhat misplaced. An adequate model of any helium atom discrete state is provided by a two-electron antisymmetric wave-function where one of the electrons is represented by the He^+ 1s orbital. This is known as the frozen-core model and suffices so long as we are only interested in one-electron excitation processes. Fortunately, these happen to be by far the most dominant. With this approximation for the helium structure the e-He system looks very similar to and not too much more difficult to calculate than the e-H system. The primary difficulty of calculation is the same for both systems, namely the treatment of the target continuum. It should be said that the fact that the frozen-core model yielded a good description of the target structure was known in the late sixties, see Cohen and McEachran (1967) for example. Just how good this model is for the purpose of electron scattering calculations has only become clear very recently (Fursa and Bray 1995, Bartschat *et al* 1996*a*).

The primary purpose of this review is to demonstrate how successfully the convergent close-coupling (CCC) method, first introduced for the e-H problem (Bray and Stelbovics 1992), has been extended (Fursa and Bray 1995) to the calculation of e-He scattering. Even though there are many examples in the literature of excellent agreement between the CCC theory and experiment, we must caution the reader that there are also outstanding systematic discrepancies with a number of independent measurements for the case of excitation from the metastable states. While it is unclear why the CCC theory would yield correct results for excitation of the ground state but not for the simultaneously obtained excitation of the metastable states, it is most disturbing to find the CCC theory yielding substantially lower results than experiments for electron scattering from the 2^3S helium state.

This work is aimed at the reader who is already familiar with the general concepts in electron-atom scattering, but is not particularly interested in immediate technical detail. In section 2 we give the outline of the CCC theory concentrating on how the close-coupling formalism is used to yield simultaneously discrete excitation and ionisation

information, and how it relates to other electron-atom scattering theories. Section 3 gives relations used to obtain, from the CCC scattering amplitudes, the data presented in the figures. This is followed by section 4 where we discuss electron-impact excitation (to $n \leq 3$ levels) and ionisation of the helium ground state. In section 5 we consider electron impact excitation (to $n \leq 4$ levels) and ionisation of the helium metastable $2^{3,1}$S states. Finally, the conclusions and future directions are given in section 6.

2. Theory

Let us begin with a general approach to electron–helium scattering. We do not wish to repeat here most of the technical detail given earlier (Fursa and Bray 1995). Instead, we would like to just give an overview that may be used to make clear the major differences between various theoretical approaches, and show how the CCC theory simultaneously yields results for discrete and ionisation processes.

Suppose we obtain the target wave functions ϕ_n by diagonalising the target Hamiltonian H_t in some explicitly antisymmetric two-electron basis of size N with square-integrable one-electron orbitals, i.e.

$$\langle \phi_f^N | H_t | \phi_i^N \rangle = \epsilon_f^N \delta_{fi}. \tag{1}$$

Thus obtained (two-electron) pseudostates ϕ_n^N, $n = 1, \ldots, N$ have a formal dependence on the basis size N, but if the basis is chosen appropriately we can assume that $\langle \phi_n^N | \phi_n \rangle \approx 1$, $\epsilon_n^N \approx \epsilon_n$ for the physical states ($H_t|\phi_n\rangle = \epsilon_n|\phi_n\rangle$) of interest. In addition, the remaining of the N states form a representation of the higher discrete target states and the target continuum. These may be combined together to define the projection operator

$$I^N = \sum_{n=1}^{N} |\phi_n^N\rangle\langle\phi_n^N|, \tag{2}$$

which will be used to form the close-coupling equations. We desire that the basis be constructed in such a way that $\lim_{N\to\infty} I^N = I$, the true target-space identity operator.

To obtain e-He scattering information we would like to know the T matrix for the $i \to f$ transition

$$\langle \Phi_f | T | \Phi_i \rangle = \langle \Phi_f | H - E | \Psi_i^{(+)} \rangle. \tag{3}$$

Here Φ_f and Φ_i are the (three-electron) final and initial channel functions, $\Psi_i^{(+)}$ is the total wave outgoing spherical wave boundary conditions, H and E are the total Hamiltonian (acting to the left) and energy, respectively. For computational convenience we write

$$|\Psi_i^{(+)}\rangle = (1 - P_{rs})|\psi_i^{(+)}\rangle, \tag{4}$$

where the use of the space and spin exchange operator P_{rs} allows us to work with a non-symmetrised function ψ_i, though at the cost of non-uniqueness (Stelbovics 1990). The N-state approximation to the true T matrix (3) we define by

$$\langle \Phi_f | T^N | \Phi_i \rangle = \langle \Phi_f I^N | (H - E)(1 - P_{rs}) | I^N \psi_i^{(+)} \rangle. \tag{5}$$

The introduction of the projection operators I^N allows us to unambiguously define the channel functions for both discrete excitation (this has never been a problem) and also ionisation. They ensure that asymptotically only the projectile-space electron is allowed to exit the scattering system. Hence, the asymptotic (channel) Hamiltonian K we write as

$$K = K_0 + H_t, \tag{6}$$

where K_0 is the one-electron projectile-space kinetic energy operator, and the channel functions, eigenfunctions of K, as

$$|\Phi_n\rangle = |\phi_n \mathbf{k}_n\rangle. \tag{7}$$

We use the discrete notation for the target eigenstates $|\phi_n\rangle$ to represent both the discrete and continuum target states. In either case, if the final target state energy ϵ_f is the same as ϵ_n^N for say $n = f$, then (5) becomes

$$\langle \Phi_f | T^N | \Phi_i \rangle \approx \langle \phi_f | \phi_f^N \rangle \langle \mathbf{k}_f \phi_f^N | V - (H - E) P_{rs} | I^N \psi_i^{(+)} \rangle \tag{8}$$

$$= \langle \phi_f | \phi_f^N \rangle T_{fi}^N, \tag{9}$$

where $V = H - K$. The T-matrix elements T_{fi}^N arise upon solution of the close-coupling equations. These are well-defined once the target-space expansion states have been obtained in (1) and the total energy E specified. See Fursa and Bray (1995) and Bray and Fursa (1996*a*) for detailed discussion.

From (9) it is clear that after the T_{fi}^N have been obtained, the scattering amplitudes for discrete transitions ($\langle \phi_f | \phi_f^N \rangle \approx 1$) and ionisation may be readily calculated. Convergence is checked by simply increasing N. In the case of ionisation, obtaining convergence in (9) is particularly noteworthy as $\lim_{N\to\infty} \langle \phi_f | \phi_f^N \rangle = \infty$.

Equation (8) may be used to outline the difference between the CCC and other approaches to the calculation of electron-atom scattering. For example, standard close-coupling (CC) methods use only the discrete states in the definition of I^N, thereby ignoring the target continuum. Pseudostate methods are very similar to the CCC method, but are somewhat less systematic in the definition of I^N and have typically been applied with much smaller N. Coupled-channel optical (CCO) methods use just a few discrete states (P-space) in the definition of I^N, but the effect of the remaining states (Q-space) is approximated by adding to V a complex nonlocal polarization potential V^Q. Distorted-wave methods approximate $|I^N \psi_i^{(+)}\rangle$ by $|\phi_i \mathbf{k}_i^{(+)}\rangle$, where $\mathbf{k}_i^{(+)}$ is a distorted wave.

Generally, for e-He excitation, the R-matrix implementation of the CC method as used recently by Fon *et al* (1995) works well at energies below the ionisation threshold, though not for elastic scattering. The R-matrix with pseudostates (RMPS) method (Bartschat *et al* 1996*a*), however, treats the target continuum via a square-integrable approach and has yielded results comparable to those of the CCC method. The CCO method of McCarthy *et al* (1991) makes approximations in the treatment of the target continuum and exchange matrix elements. Unlike CC methods, it does yield good elastic cross sections (Brunger *et al* 1992), but has difficulties with exchange transitions. The distorted-wave methods, being high-energy approximations, are generally not reliable below approximately 100 eV. They exhibit a strong sensitivity to the choice of the distorting potentials (Madison 1979) and perform poorly for exchange transitions. For direct transitions, the first-order many-body theory (FOMBT) of Cartwright *et al* (1992) and the distorted-wave approximations (DWA) of Bartschat and Madison (1988) are often quite accurate.

In passing, we note that the variational calculations of low-energy elastic scattering by Nesbet (1979) have withstood the test of time and have provided a very useful standard against which more-complicated theories may be tested.

3. Physical observables

In this section we discuss how various cross sections and angular correlation parameters measured in experiment may be calculated using the T-matrix elements arising from the CCC calculations. This section is presented for completeness and for ease of reference.

3.1. Cross sections

The CCC calculations yield, for discrete transition $i \to f$, reduced T-matrix elements, which depend on the total spin S, parity Π and partial wave of total orbital angular momentum J. These are related to the scattering amplitudes in the collision frame, where the quantization axis is along the incident projectile direction, by

$$f^S_{m_f m_i}(\theta,\varphi) = \frac{1}{\sqrt{4\pi}}\frac{1}{\sqrt{2l_i+1}}\sqrt{\frac{k_i}{k_f}}\sum_{L_f,L_i,J}\sqrt{2L_i+1}C^{m_i-m_f\,m_f\,m_i}_{L_f\quad l_f\quad J} \times C^{0\;m_i m_i}_{L_i l_i\;J} T^{JS\Pi}_{l_i l_f L_i L_f} Y^{L_f}_{m_i-m_f}(\theta,\varphi), \tag{10}$$

where l and m, are the atom orbital angular momentum and its projection, while k and L are and projectile linear and orbital angular momenta. The spherical polar angles of the detected electron are θ and φ. The T-matrix elements, and thus the scattering amplitudes, depend on the basis size N of the calculation. For clarity of notation we do not include the N index, but assume that the calculations have been performed with a sufficiently-large N so that convergence to a required accuracy has been attained.

All experimentally-observable quantities may be related to the scattering amplitudes. If the initial state of the helium atom is a singlet state then only spin channel $S = 1/2$ (doublet channel) is possible. The differential cross section (DCS) is then given by averaging over magnetic sublevels of the initial state orbital angular momentum l_i, via factor $1/\sqrt{2l_i+1}$ in (10), and summation over magnetic sublevels of the final state orbital angular momentum

$$\frac{d\sigma}{d\Omega}^S = \sum_{m_f,m_i} |f^S_{m_f m_i}|^2. \tag{11}$$

If the initial state of the helium atom is a triplet state then an additional independent spin channel $S = 3/2$ (quartet channel) is possible. The spin-resolved differential cross section is given by (11). The spin-averaged differential cross section is obtained by averaging over magnetic sublevels of the helium atom initial spin $s_i = 1$ and two possible spin projections of the incident electron, as well as summation over the total spin S and its projections

$$\frac{d\sigma}{d\Omega} = \frac{1}{2(2s_i+1)}\sum_S (2S+1)\frac{d\sigma}{d\Omega}^S = \frac{1}{6}\left(2\frac{d\sigma}{d\Omega}^{1/2} + 4\frac{d\sigma}{d\Omega}^{3/2}\right). \tag{12}$$

The ratio of the quartet to doublet differential cross sections

$$r = \frac{d\sigma}{d\Omega}^{3/2} \Big/ \frac{d\sigma}{d\Omega}^{1/2} \tag{13}$$

is used to define an exchange asymmetry via

$$A_{\rm ex} = \frac{1-r}{1+2r}, \tag{14}$$

which has the advantage of always being finite. For pure doublet scattering $A_{\rm ex} = 1$ ($r = 0$) while for pure quartet scattering $A_{\rm ex} = -1/2$ ($r = \infty$).

The integrated cross section σ may be found by integration of the corresponding differential cross section over the scattering angles or by summing the partial cross sections. The total cross section $\sigma_{\rm t}$ from initial state i may be obtained by summing the individual integrated cross sections for each state ($f = 1, \ldots, N$) used in the close-coupling expansion, or utilizing the unitarity of the close-coupling formalism by using the optical theorem. The total ionisation cross section (TICS) is defined by

$$\sigma_{\rm i} = \sigma_{\rm t} - \sigma_{\rm nb}, \tag{15}$$

where $\sigma_{\rm nb}$ is the total non-breakup (elastic plus bound state excitations) cross section obtained by summing the integrated cross sections for negative-energy (ϵ^N_f) states.

3.2. Electron-impact coherence parameters (EICPs)

Measurements of differential cross sections allow for testing of only the magnitudes of the scattering amplitudes summed over the magnetic sublevels. Much more information

about the scattering process (namely, the relative phases between the scattering amplitudes) can be obtained if the scattered electrons are measured in coincidence with dipole radiation arising from atoms excited by the electron impact. Such measurements determine parameters related to the parameterization of the dipole photon polarization density matrix (Blum 1981), and are known as the Stokes parameters P_1, P_2, P_3.

Parameters P_1 and P_2 are the degrees of linear polarization and P_3 is the degree of circular polarization of the radiation propagating perpendicularly to the scattering plane. These three Stokes parameters, together with the DCS, are sufficient to completely describe excitation of helium P-states from the ground state. To characterize excitation of D-states an additional measurement of the degree of linear polarization of the radiation propagating in the scattering plane may be performed. This is the Stokes parameter P_4. However, this still leaves the characterization of D-state excitation incomplete.

The Stokes parameters P_1, P_2, P_3, P_4 may be written in terms of the state multipoles T_{kq} (Blum 1981, Andersen *et al* 1988)

$$P_1 = \frac{\alpha_2(T_{22} - \sqrt{\frac{3}{2}}T_{20})/2}{T_{00} - \frac{\alpha_2}{2}(T_{22} + T_{20}/\sqrt{6})}, \tag{16}$$

$$P_2 = \frac{\alpha_2 T_{21}}{T_{00} - \frac{\alpha_2}{2}(T_{22} + T_{20}/\sqrt{6})}, \tag{17}$$

$$P_3 = -\frac{\alpha_1 i T_{11}}{T_{00} - \frac{\alpha_2}{2}(T_{22} + T_{20}/\sqrt{6})}, \tag{18}$$

$$P_4 = -\frac{\alpha_2(T_{22} + \sqrt{\frac{3}{2}}T_{20})/2}{T_{00} + \frac{\alpha_2}{2}(T_{22} - T_{20}/\sqrt{6})}, \tag{19}$$

where the coefficients α_k are

$$\alpha_k = 3\sqrt{2l_1+1}(-1)^{l_1+l_2+k+1}\begin{Bmatrix} 1 & l_1 & l_2 \\ l_1 & 1 & k \end{Bmatrix}. \tag{20}$$

Here $l_1 = l_f$ and $l_2 = l_f - 1$ for dipole photon deexcitation. For scattering to a P-state, $l_1 = l_f = 1$, $l_2 = 0$, and in this case $\alpha_1 = \alpha_2 = \sqrt{3}$. For scattering to a D-state $l_1 = l_f = 2$, $l_2 = 1$, and in this case $\alpha_1 = 3/2$, $\alpha_2 = \sqrt{21/20}$. The spin-averaged state multipoles T_{kq} are

$$T_{kq} = \sum_{m,m'} (-1)^{l_f - m} C^{m'-mq}_{l_f\ l_f\ k} \rho_{mm'}, \tag{21}$$

where the spin-averaged density matrix is

$$\rho_{mm'} = (\rho^{1/2}_{mm'} + 2r\rho^{3/2}_{mm'})/(1+2r). \tag{22}$$

The above spin-resolved density matrix $\rho^S_{mm'}$ of the final state, normalized to unit trace, is given by (Blum 1981)

$$\rho^S_{mm'} = \sum_{m_i} \frac{f^S_{mm_i} f^{S*}_{m'm_i}}{\frac{d\sigma^S}{d\Omega}}. \tag{23}$$

The state multipoles are normalized to have $T_{00} = 1/\sqrt{2l_f+1}$. The spin-resolved state multipoles T^S_{kq} are obtained by using the spin-resolved density matrix in (21). Spin-resolved counterparts to the Stokes parameters may be obtained by restoring the total spin S index to the state multipoles T_{kq} in (16–19). It is also clear that Eqs. (16-19) can be inverted and the state multipoles T_{kq} can be expressed via Stokes parameters.

A more physical description of the atom charge cloud is provided by the alignment, orientation, and coherence parameters (Andersen *et al* 1988). The linear polarization of the atomic charge cloud is

$$P_\ell = (P_1^2 + P_2^2)^{1/2}, \tag{24}$$

the alignment angle relative to the z axis of the collision frame is

$$\gamma = \arg(P_1 + iP_2)/2, \tag{25}$$

the degree of polarization (total coherence) is

$$P = (P_1^2 + P_2^2 + P_3^2)^{1/2}, \tag{26}$$

and the angular momentum transferred to the atom perpendicular to the scattering plane is

$$L_\perp = \sqrt{\frac{2(2l_f+1)(l_f+1)l_f}{3}}\ iT_{11} = -\frac{\sqrt{3(l_f+1)l_f/2}}{\alpha_1} I_z P_3, \tag{27}$$

where I_z is proportional to the detected radiation intensity in the direction perpendicular to the scattering plane.

$$I_z = \frac{2}{3T_{00}}(T_{00} - \frac{\alpha_2}{2}(T_{22} + T_{20}/\sqrt{6})) = -\frac{2(P_4+1)}{4-(P_1-1)(P_4-1)}. \tag{28}$$

For S to P excitation ($l_i = 0$, $l_f = 1$) (16–18) can be simplified. The symmetry property of the scattering amplitudes $f^S_{10} = -f^S_{-10}$ results in the additional relation for the state multipoles (Hertel and Stoll 1977)

$$T_{20}/\sqrt{6} + T_{22} = -1/3, \tag{29}$$

and the Stokes parameters are then given by

$$P_1 = 1 + 4T_{22}, \tag{30}$$

$$P_2 = 2T_{21}, \tag{31}$$

$$P_3 = -2iT_{11} = -L_\perp. \tag{32}$$

In this case measurement of the three Stokes parameters and the DCS allows the state multipoles T^S_{kq}, and consequently the scattering amplitudes f^S_{m0}, to be determined unambiguously (up to an overall phase in the case of scattering from ^{3}S states). There is complete coherence ($P^S = 1$) in both the doublet and quartet channels. However, when scattering from a ^{3}S state, the spin-averaged P is not equal to unity and its deviation from unity is a measure of exchange scattering, though not a very sensitive one.

The study of S- to D-state excitation usually involves the definition of one more parameter. It is convenient to use the natural-frame density-matrix element (Andersen *et al* 1988)

$$\rho^n_{00} = \frac{1}{2} + \frac{\sqrt{21}}{4}(T_{22} + \frac{T_{20}}{\sqrt{6}}). \tag{33}$$

It can be expressed in terms of the Stokes parameters as,

$$\rho^n_{00} = \frac{3}{2}(1 - I_z) = \frac{3}{2}\left(1 - \frac{2(1+P_4)}{4-(1-P_1)(1-P_4)}\right). \tag{34}$$

The complete description of D-state excitation requires state multipoles T_{kq} up to rank $k = 4$. However, measurements of the Stokes parameters $P_1, \ldots, P_4$ in the standard electron-photon coincidence experiment can yield state multipoles up to rank $k = 2$ only. The state multipoles of rank $k = 3$ and 4 can be obtained from two-photon-electron coincidence measurements, where in addition to the D $\rightarrow$ P photon being detected, the P $\rightarrow$ S photon is measured in coincidence. See the work of Mikosza *et al* (1993) and Mikosza *et al* (1996) for details.

A major complication arises for the analysis of the 3^3P and 3^3D state excitation. In these cases the spin-orbit interaction leads to a depolarisation of the radiation emitted and hence measured polarisations cannot be simply related to any description of the excited state produced in the collision. If the fine-structure splitting is large compared with the natural line width, which is true for the He 3^3P and 3^3D states, the depolarisation can be taken into account by introducing the perturbation coefficients G_k (see Blum (1981) for detailed discussion) and replacing the coefficient α_k in (16-19) by $\alpha_k G_k$.

We will denote the observed Stokes parameters by $P'_1, \ldots, P'_4$ while keeping the unprimed notation for the reduced Stokes parameters, those that would be measured if there were no depolarisation due to the spin-orbit interaction ($G_k = 1$). The observed Stokes parameters can be readily related to the reduced ones by (Crowe *et al* 1994),

$$P_i = P'_i \frac{I'_z}{\frac{2}{3}(G_2 - 1) + I'_z}, \quad i = 1, 2 \tag{35}$$

$$P_3 = (G_2/G_1)P'_3 \frac{I'_z}{\frac{2}{3}(G_2 - 1) + I'_z}, \tag{36}$$

$$P_4 = P'_4 \frac{2 - I'_z(1 - P'_1)}{\frac{2}{3}(2G_2 + 1) - I'_z(1 - P'_1)}, \tag{37}$$

where

$$I'_z = \frac{2(1+P'_4)}{4-(1-P'_1)(1-P'_4)} = G_2 I_z - \frac{2}{3}(G_2 - 1). \tag{38}$$

From the above relations it is clear that the determination of the reduced Stokes parameters generally requires the in-plane measurement of the parameter P'_4.

For the 3^3P state $G_1 = 1/2$ and $G_2 = 5/18$ and, due to (29), the relation between the observed P'_1, P'_2, P'_3 and reduced P_1, P_2, P_3 Stokes parameters simplifies to

$$P'_1 = c_1 P_1, \quad P'_2 = c_1 P_2, \quad P'_3 = c_2 P_3, \tag{39}$$

where $c_1 = 15/41$ and $c_2 = 27/41$ are the constant depolarisation coefficients. For the 3^3D state $G_1 = 43/54$ and $G_2 = 71/150$. However, the relation between the observed and the reduced Stokes parameters cannot be simplified any further and the constant depolarisation coefficients cannot be formulated.

Crowe *et al* (1994) obtained the relations (35–37) when analyzing helium 3^3D angular correlations. In fact they are valid for arbitrary orbital angular momentum of the target final and initial states. If more than one total spins are involved then the spin index needs to be restored and appropriate averaging performed. For targets with nonzero nuclear spin (eg. sodium) the hyperfine structure corrections should be taken into account when calculating the coefficients G_k (see Blum (1981) and Andersen *et al* (1988) for details).

4. Electron scattering from the helium ground state

Traditionally, the energy range of interest in atomic physics has been divided into the low (below ionisation threshold), intermediate (between one and ten times the ionisation threshold) and high (more than ten times the ionisation threshold) regions. This was done as some theories worked well in either extreme of the energy range, and none were reliable at intermediate energies. One of the primary motivations in the development of the CCC method was to devise a theory that is equally valid irrespective of the incident energy. A demonstration of this for e-He(1^1S) scattering has been given by Fursa and Bray (1995), where the energy considered ranged from 1.5 to 500 eV. Here we primarily wish to concentrate on a single energy of 30 eV. This is in the most difficult intermediate energy range, being only 5.4 eV above the ionisation threshold. Techniques that treat the target continuum via a square-integrable approach, such as our own, have to be able to demonstrate that the results are free from pseudoresonance effects. In addition, at this energy a large set of experimental data and calculations are available for comparison.

A key feature of the CCC formalism is that convergence to some accuracy in the parameter of interest needs to be demonstrated as a function of the number of states used. The CCC(69) and CCC(75) calculations (Fursa and Bray 1995) generally showed good agreement with each other, but differed visibly on some occasions. The difference between them is that the former had more S-, P- and D-states than the latter, which in addition had F-states. Here, where appropriate, we shall present results from 111-state calculations which have more S-, P- and D-states than the CCC(69), more F-states than the CCC(75) and also have G-states. Specifically, the CCC(111) results presented below were obtained with 14 ^{1}S states, 13 ^{3}S and ^{3,1}P states, 12 ^{3,1}D states, 10 ^{3,1}F states and 7 ^{3,1}G states. An implementation of such a calculation using the CCC method required in excess of 1G core memory.

We should note that in the relatively-comprehensive earlier work (Fursa and Bray 1995) there was no discussion of resonances. The CCC method is able to calculate these, and has done so in the case of e-H (Bray *et al* 1996) and e-He$^+$ (Bray *et al* 1993) scattering, however it is not best suited for such calculations. The *R*-matrix (Berrington and Kingston 1987, Sawey *et al* 1990), and preferably RMPS (Bartschat *et al* 1996*b*) or *J*-matrix methods (Konovalov and McCarthy 1995) are more-appropriate choices for investigation of threshold and resonance behaviour since they typically yield results on a fine energy mesh rather than at a single energy as is the case in the CCC method.

4.1. Elastic scattering

Elastic e-He scattering is well understood experimentally and theoretically and has been used extensively for calibration purposes in various electron-scattering applications. We would like to draw the attention of the reader to the comprehensive data set of absolute differential and integrated elastic cross sections given by Register *et al* (1980). The reported data at an impact energy range of 5 to 200 eV are in good agreement with the more-recent study by Brunger *et al* (1992) (1.5 - 50 eV).

The major difficulty in calculating e-He elastic cross sections is to fully account for the atomic-static dipole polarisability, a significant part of which comes from the continuum. The pseudostate technique has been successfully used in the *R*-matrix method by O'Malley *et al* (1979) and Fon, Berrington and Hibbert (1981), and variational formalism by Nesbet (1979). Perturbative methods account for the dipole polarisability by going to second order, subject to approximations. For example, the closure approximation was used in the second-order method of Winters *et al* (1974), in the eikonal-Born method of Byron and Joachain (1977), and in the distorted-wave second Born approximation of Dewangan and Walters (1977). A pseudostate technique has been used in the second-order many-body theory method by Scott and Taylor (1979). The polarised-orbital method was also applied to calculate elastic scattering by LaBahn and Callaway (1970).

Generally the agreement between above theory and experiment is very good. However, most of these methods have been limited to the calculation of elastic scattering only. More-sophisticated general electron-atom scattering methods (CCO, CCC, RMPS) have been developed later and applied to the calculation of elastic scattering. These methods have been able to improve agreement with experiment in the few places where it was not perfect.

In figure 1 we present the CCC calculations (Fursa and Bray 1995) of the e-He elastic DCS at low and intermediate energies. The results at 30 eV have been replaced by those of the present 111-state calculation. The agreement with the measurements of Brunger *et al* (1992) and Register *et al* (1980) is quantitative at all incident electron energies. Where available, the results of the variational calculations of Nesbet (1979) (5 and 18 eV), *R*-matrix calculations of Fon, Berrington and Hibbert (1981) and the RMPS calculations (Bartschat *et al* 1996*a*) (30 and 50 eV) are presented for comparison. The variational, *R*-matrix and RMPS calculations have a very accurate ground state with ^{1}P pseudostates to account for the helium dipole polarisability. On the other hand, the CCC calculations differ in that the simpler frozen-core model of the helium atom yields a less accurate ground state. However, the agreement between the results of all four methods is very good, specially below the first excitation threshold. This indicates that the frozen-core model is sufficiently accurate for the description of elastic scattering. Since the largest error in the description of the helium bound states using the frozen-core model occurs in the ground state, accurate results for elastic scattering are a good indication of the reliability of the model for inelastic scattering (Fursa and Bray 1995).

4.2. Excitation of n=2 states

We now turn to the discussion of excitation cross sections of the $2^{1,3}$S and $2^{1,3}$P states and EICPs of the 2^1P state. Although a great body of measurements are available over a wide range of incident electron energies, the agreement between them is not always perfect. Similarly, calculations including DWBA (Bartschat and Madison 1988), FOMBT (Csanak and Cartwright 1988), *R*-matrix (Fon *et al* 1979, Freitas *et al* 1984, Berrington and Kingston 1987, Sawey *et al* 1990), and CCO (McCarthy *et al* 1991, Brunger *et al* 1992) methods often disagree with each other and the measurements. However, application of the CCC theory (Fursa and Bray 1995), new measurements (Röder *et al* 1996*a*), and most recent RMPS (Bartschat *et al* 1996*a*) calculations has changed the situation substantially for the better.

The current status of theory and experiment is summarised in figure 2, where the differential cross sections are presented at 30 eV incident electron energy. For optically-forbidden transitions ($2^{1,3}S, 2^3$P) the results of the theoretical methods are

often very different. At this low energy the FOMBT method is quite unreliable. The 29-state R-matrix (RM(29)) calculation is in better agreement with experiment than the FOMBT results. However, only the CCC (111 states) and RMPS results are in good agreement with each other and experiment. For the 2^3P excitation there are some shape differences between the CCC and RMPS results as well as between the experimental data of Brunger *et al* (1990) and Trajmar *et al* (1992). However, the recent relative measurements of Röder *et al* (1996*a*) are in very good agreement with the CCC results when suitably normalized. The small statistical uncertainty (<5 %) of the latter measurements suggests that the CCC results may be the most accurate. As in the case of elastic scattering, the application of the RMPS theory confirms the conclusion that treating the target continuum is more important than improving the frozen-core structure model.

Experimental and theoretical results for the optically-allowed 2^1P excitation differential cross sections show little variation in shape though the magnitude does vary. A stronger test of the scattering theories is provided by the EICPs determined from the electron-photon coincidence measurements, see section 3.2. In figure 3 we present the 2^1P EICPs at 30 eV. The agreement between the CCC results and experiments is good. This is also the case for the R-matrix calculations with (RMPS) and without (RM(29)) the treatment of the target continuum. This indicates that for this excitation the exclusion of the target continuum does not result in a substantial error for the EICPs. However, the results of the FOMBT are very different and disagree with experiment and the other calculations.

4.3. Excitation of n=3 states

Differential cross sections for the $3^{1,3}$S and $3^{1,3}$P states at 30 eV are presented in figure 4. Here the situation is very similar to the case of $n = 2$ excitation. The CCC results are in good agreement with experiment for all transitions. The FOMBT is inadequate for the optically-forbidden transitions, but is in good agreement with experiment for the optically-allowed 3^1P excitation. The RM(29) calculation treats only the target discrete subspace, and exhibits substantial problems. Even for the optically-allowed 3^1P excitation the R-matrix results are systematically too high. This suggests that the treatment of higher discrete excited and continuum states becomes progressively more important with increasing excitation energy of the observed state. We look forward to the extension of the RMPS method to the $n = 3$ states.

Excitations of the 3^1P and $3^{1,3}$D states are very difficult to resolve due to their very small energy separation. Recently Khakoo *et al* (1995) have performed the first measurements of the 3^1P DCS that are resolved from the $3^{1,3}$D levels using the electron-photon coincidence technique. The new data are in very good shape agreement with the

CCC theory, but are somewhat systematically higher. For this reason also presented in figure 4 are the measurements of Chutjian and Thomas (1975) and Trajmar *et al* (1992) of the summed DCS for the 3^1P and $3^{1,3}$D states with the CCC theoretical DCS for $3^{1,3}$D states (see figure 7) subtracted. Theory indicates that excitation of the 3^1P state is dominant for scattering angles $\theta < 60°$, and so somewhat better agreement with the earlier measurements is encouraging.

The 3^1P angular correlations are presented in figure 5. The EICPs $L_\perp$ and γ and Stokes parameters P_1 and P_2 reported by Neill and Crowe (1988) and Neill *et al* (1989) are compared with results of the CCC, 19- and 29-state R-matrix, and DW calculations. The DW results are in poor agreement with the experiment. Similar to the FOMBT the DW method is a high-energy approximation and is not accurate at such a low energy. The R-matrix methods have achieved good convergence, but to the wrong result in the case γ at intermediate electron scattering angles. The alignment angle γ is a derived parameter related to the observed Stokes parameters ($\gamma = \texttt{ATAN2}(P_2, P_1)/2$). It is more instructive to compare with the originally-measured P_1 and P_2 parameters. Whereas agreement with the P_2 data is good there are some problems in the case of P_1. Some variation between the two reported measurements indicates the difficulty of the experiment.

In figure 6 we present the EICPs for the 3^3P state at 30 eV. The measured radiation in this case is depolarised (see (39) for the relation between the measured and the reduced Stokes parameters). Both the CCC and R-matrix results are similar and show satisfactory agreement with experiment.

We now turn to the discussion of the $3^{1,3}$D states. No DCS measurements have been reported due to the above-mentioned problem of resolving D-states from the 3^1P state. In figure 7 we compare the CCC(111) results with the CCC(75) and with the DW calculations of Bartschat and Madison (1988). The two CCC calculations show good convergence. The two DW results are very different from each other, indicating the large dependence on the choice of the distorting potential, with neither choice agreeing with the CCC results.

Extensive electron-photon coincidence measurements are available for electron impact excitation of the helium $3^{1,3}$D states. In figure 8 we present the EICPs and Stokes parameters for the 3^1D state at 30 eV. We observe generally good convergence of the CCC results and good agreement with experiment of Donnelly *et al* (1994). The DW results of Bartschat and Madison (1988) are in poor agreement with experiment and the CCC results. For Stokes parameters P_1 and P_2 the experiment and CCC results are in relatively good agreement. However, this is not the case for the alignment angle γ. The apparent disagreement between the CCC results and experiment here is an artifact of the definition (25) of the alignment angle γ.

The 3^3D state EICPs and measured Stokes parameters (P_1'-P_4' are presented in

figure 9. The latter parameters are affected by fine structure depolarisation (see Eq. (35-37)). Examining the CCC(111) and CCC(75) calculations we observe good convergence and agreement with experiment. This indicates that the effect of the G-states, included in the CCC(111) calculation, is small and that there is no need to include target states with higher angular momentum.

4.4. Ionisation

Historically, the close-coupling formalism was designed and used to calculate elastic and bound-state-excitation processes. The introduction of pseudostates into the close-coupling method allows for an estimate of the total ionisation cross section (TICS). The TICS is then obtained as the difference between the total and total nonbreakup cross sections (15) or, alternatively, by summing integrated cross sections for positive energy pseudostates.

One of the first examples of the success of the CCC theory was its application to the calculation of TICS in the case of e-H scattering (Bray and Stelbovics 1993), where remarkable agreement was found with experiment. This has since been demonstrated for the e-He system (Fursa and Bray 1995), given in figure 10. We compare the results of the CCC(69) calculations with experiment of Montague *et al* (1984) and Born calculation of McGuire (1971) and distorted-wave-with-exchange (DWE) calculation of Younger (1981). The CCC results are in good agreement with experiment and superior to the Born and DWE calculations in the intermediate energy region. At high energies ($\geq$ 500 eV) the CCC results underestimate the TICS due to the use of the frozen-core model (only one-electron ionisation without He^+ excitations is allowed).

It is quite remarkable that the CCC(69) calculation, which has only target states with maximum orbital angular momentum $l_{max} = 2$, is in such a good agreement with experiment. Interestingly, unitarity of the CC formalism ensures rapid convergence with l_{max} without requiring convergence in the individual l-dependent contributions (Bray 1994). However, in order to calculate differential ionisation cross sections we do require convergence in all of the contributions.

The ability to correctly predict the TICS invites investigation to determine whether the CCC method yields correct differential distributions in the case of ionisation. This, at first glance, is an odd thing to do because the method formally allows for only a single projectile-space electron to be in the true continuum. All other electrons are treated by square-integrable functions. Curran and Walters (1987) and Curran *et al* (1991) took the approach that the pseudostate expansion yields an accurate total wave function, and generated triple differential ionisation cross sections using this wave function. This approach leads to nonexistent integrals that arise due to an inconsistent treatment of the total wave function and the asymptotic two-electron continuum states. We avoid

this problem by using the target-space projection operator I^N on both sides of (5), and then directly relate the T-matrix element for excitation of a positive-energy pseudostate to the ionisation channel via (9). Detailed discussion of these issues together with the explicit definitions of the CCC ionisation amplitudes has been given by Bray and Fursa (1996*a*) and will not be repeated here.

Application of the CCC method to differential ionisation is still in its infancy. The first application was for e-H ionisation at 54.4 and 150 eV (Bray *et al* 1994), where very good agreement was found with the experimental data, available only for the highly asymmetric energy sharing region. A more thorough test of the CCC theory may be performed by comparison with the much more numerous e-He ionisation data. For example, at 100 eV (Bray and Fursa 1996*b*) a single CCC calculation has yielded good agreement with experiment for elastic and excitation (to $n \leq 3$) DCS, and with the ionisation single (SDCS), double (DDCS), and triple (TDCS) differential cross sections. The CCC calculations had $l_{max} = 3$ and the TDCS measurements of Röder *et al* (1995) in the standard coplanar geometry for ejected electron energy of 4 eV were reproduced essentially quantitatively. The DDCS and SDCS data of Müller-Fiedler *et al* (1986) are available not only for the asymmetric but for the whole kinematical region. Given the relatively small $l_{max} = 3$ it was particularly encouraging to find good agreement with all of the 100 eV data of Müller-Fiedler *et al* (1986), even in the case of both outgoing electrons having nearly 40 eV.

A detailed comparison of the CCC results and experiment for incident electron energies above 100 eV has been given (Bray and Fursa 1996*a*). We believe that for these energies the CCC method is able to yield accurate ionisation cross sections for all energy sharing combinations of the outgoing electrons. For the purpose of illustration we present our results at 600 eV. Note that at such high energies many other approaches to ionisation work well (Byron *et al* 1986, Furtado and O'Mahony 1988, Brauner *et al* 1991, Franz and Altick 1992, Jones *et al* 1993, Biswas and Sinha 1995). At such a high energy exchange may be dropped from the CCC calculations and so only singlet states need be included in the close-coupling expansion. In figure 11 we present results of the CCC(51) no-exchange calculation with $l_{max} = 5$. We can see very good agreement with coplanar TDCS measurements of Jung *et al* (1985) performed at a number of ejected-electron energies E_B (2.5, 5, and 10 eV) and a number of fixed angles of the fast electron θ_A (2°, 6°, 8°, and 10°). In figure 12 we compare the CCC(51) results with the DDCS measurements of Müller-Fiedler *et al* (1986). We find generally good agreement except for the largest ejected-electron energy (40 eV). The normalization of the measured DDCS by extrapolation to the optical oscillator strength is least reliable for the largest momentum transfer and may be the reason for at least some of the observed discrepancy between the CCC results and experiment.

To our mind the really interesting test of the CCC approach to ionisation is at

low incident energies. This is because in this case electron-electron correlation is particularly important and is substantial at greater distances from the nucleus. Now, we already know that the CCC method obtains accurate results for elastic and excitation processes, as well as the total ionisation cross section (Fursa and Bray 1995). What about differential ionisation cross sections at low to intermediate energies?

In figure 13 we present a three-dimensional plot of the coplanar TDCS for 40 eV incident-electron energy and 4 eV slow-electron energy. Detailed discussion and comparison with experiment (including two-dimensional cuts for fixed angle of the fast and slow electrons) has been given by Röder *et al* (1996*b*). For this kinematic region forward scattering of the fast electron with backward scattering of the slow electron is by far the dominant process. Here, as well as at 50 eV incident electron energy (Röder *et al* 1996*c*), the CCC method obtains good agreement with experiment in the asymmetric kinematical region. However, as the energies of the outgoing electron come closer we find that the CCC theory yields magnitudes that are systematically lower than experiment, while still keeping good angular profiles (Röder *et al* 1996*c*, Röder *et al* 1997*a*, Röder *et al* 1997*b*). This rather surprising result is currently under intense investigation.

5. Electron scattering from the helium metastable states

A great strength of the close-coupling methods is the ability to obtain from a single calculation the scattering results for transitions between various initial and final states. The reliability of the CCC theory should be independent of the initial state. The excellent agreement the CCC theory has generally attained with measurements of the e-He(1^1S) system should translate directly to good agreement with measurements of the e-He($2^{3,1}$S) scattering systems. Unfortunately this is not the case. We have found systematic discrepancy between the CCC results and measurements of the differential (Müller-Fiedler *et al* 1984) and integral (Dixon *et al* 1976, Lagus *et al* 1996) cross sections for excitation of the 2^3S helium metastable state. Of particular concern is the fact that the CCC theory typically predicts a factor of two or so lower than the various independent experiments.

Scattering from the helium 2^3S state is a little different to scattering from the ground state or 2^1S states. In addition to the total spin $S = 1/2$ (all that is necessary for singlet states) the total spin now also takes on the additional value of $S = 3/2$. In parallel to scattering from quasi-one-electron targets, two independent calculations are now required, one for each of the total spin cases. The calculated observables have to be appropriately spin averaged (12) when compared with spin-unresolved experimental data. Note that the total spin $S = 3/2$ case requires significantly less computer time because only triplet ($s = 1$) target states are included in the close-coupling calculations.

In performing e-He(1^1S,$2^{3,1}$S) calculations, we have a constant total energy E in all channels. Denoting by ϵ_n the projectile energy relative to state n with energy ϵ_n, we have

$$\begin{aligned} E &= \varepsilon_{1^1\mathrm{S}} + \epsilon_{1^1\mathrm{S}} \\ &= \varepsilon_{2^1\mathrm{S}} + \epsilon_{2^1\mathrm{S}} \\ &= \varepsilon_{2^3\mathrm{S}} + \epsilon_{2^3\mathrm{S}}. \end{aligned} \tag{40}$$

Therefore, a single calculation for a total energy E leads to results with different incident projectile energies corresponding to different incident target states.

5.1. *Excitation*

The DCS for electron impact excitation of the helium 2^3S state (to $n \leq 4$ triplet states) have been measured by Müller-Fiedler *et al* (1984) at a number of fixed outgoing-electron energies (15, 20 and 30 eV). In figure 14 we present experimental and theoretical results at 20 eV outgoing electron energy (see Bray and Fursa (1995) for comparison at other energies). The fixed outgoing electron energy implies different incident energies for each excitation channel and formally requires a separate calculation. However the energy difference between helium states excited from the 2^3S state is relatively small and the cross sections change slowly with energy. Therefore we make an insignificant error by comparing with a single CCC calculation at the incident energy of 21 eV relative to the 2^3S state. This energy leads to the outgoing energy of approximately 20 eV for each of the excitation channels. It also corresponds to 40 eV incident energy relative to the helium ground state, where there are extensive experimental data in very good agreement with the CCC theory (Fursa and Bray 1995). Examining figure 14 we observe that the experimental results of Müller-Fiedler *et al* (1984) are systematically higher than the CCC results for all transitions, but angular distributions are generally in good qualitative agreement. The present 40 eV CCC(111) calculation uses the same number of states in each target symmetry as the one used at 30 eV. Convergence is clearly established by comparison with the CCC(75) results. Also presented are the FOMBT and DWA data of Cartwright and Csanak (1995). It is interesting to note that for 3^3P state excitation there is a structure in the small-angle differential cross section which is present in the CCC results as well as in the results of various distorted-wave methods (Flannery and McCann 1975, Mathur *et al* 1987, Cartwright and Csanak 1995, Verma *et al* 1995), but not in the experiment. Clearly, the most disturbing aspect of the comparison of theory and experiment is the discrepancy in magnitude. In passing, we note that there are also measurements of the superelastic DCS of the 2^3S helium state (Jacka *et al* 1995). Whereas these show excellent angular agreement with the CCC theory they are not absolute and so do not help us to resolve the magnitude problems.

Extensive application of the CCC method to the calculation of e-He($2^{3,1}$S) excitation cross sections has been reported by de Heer *et al* (1995). There the CCC method was used to establish the preferred data set for use in fusion research. Comparison with the many available theories may be found there. In figure 15 the integrated cross sections for excitation of the 3^3S, 3^3P, 3^3D, and 4^3D states from the 2^3S helium state are presented. Comparison is made with the measurements of the apparent (direct plus cascades) cross sections by Rall *et al* (1989) (for the 3^3P state the direct cross section is presented) and with the measurements of the direct cross sections by Lagus *et al* (1996). The results of the CCC(69), CCC(75) and CCC(111) calculations are presented together with the FBA calculations (Kim and Inokuti 1969, Briggs and Kim 1971) and the 11-state R-matrix calculations (Berrington *et al* 1985).

At higher energies the CCC and FBA calculations converge together for all optically-forbidden transitions. However the experimental data of Lagus *et al* (1996) are systematically higher than the theoretical results. For the optically-allowed 3^3P excitation we observe a constant difference at high energies between the FBA and CCC results. Here the 3^3P excitation cross section is proportional to the optical oscillator strength for the 2^3S-3^3P transition. The difference between the CCC and FBA results is, therefore, due to the difference between the frozen-core model of helium structure that has been used in the CCC calculations and the highly-accurate Hylleraas-type wave functions (Weiss 1967) employed in the FBA calculations.

As the incident electron energy decreases we can see the growing difference between CCC(75) and CCC(69) results. The difference is smallest for 3^3S excitation, becomes noticeable for the 3^3P state, and is the largest for 3^3D and 4^3D states. This is consistent with the effect of inclusion of F-states in the CCC(75) calculation which are absent in the CCC(69) calculation. The CCC(69) results generally overestimate the cross sections and the CCC(75) results should be considered as more accurate. The CCC(111) calculations presented at two incident electron energies of 16.5 eV and 21 eV (obtained from the e-He(1^1S) calculations at 30 and 40 eV) indicate that the inclusion of the G-states is negligible on the considered transitions.

The RM(11) calculations have only $n \leq 3$ shell states included. It therefore overestimates the cross section for $n = 3$ states due to the absence of the $n = 4$ and higher-lying S-, P-, D-, F-states and the continuum. The CCC and R-matrix results converge together at the lowest available common energy point just below $n = 4$ excitation thresholds (≈ 3.8 eV). Similarly, the FBA calculations must be seen as being too high at the intermediate and low energies.

5.2. *Ionisation*

One aspect of particular interest to us is comparison with experiment for the case of total ionisation. We have seen that the CCC method yields good agreement with experiment in the case e-He(1^1S) ionisation. In figure 16 we present the results for ionisation cross sections (total (TICS) and spin asymmetry (A_i)) of the helium 2^3S state. The difference between the 75- and 111-state calculations indicates the minimal importance of G-states in this process. Although convergence in the TICS is not of the same accuracy as in the case of ionisation of the ground state, the large discrepancy with the experiment of Dixon *et al* (1976) is not due to convergence problems. At the higher energies the Born calculations of Ton-That *et al* (1977), Born-Ochkur calculations of Peach (Dixon *et al* 1976), and the CCC calculations converge and lie considerably below the experimental data.

The only theoretical calculation consistent with the experimental TICS results at high energies is the Bethe-Born calculation of Briggs and Kim (1971). However, it and the experiment do not reach the Born limits as calculated by Ton-That *et al* (1977) and Peach (Dixon *et al* 1976) even at 1000 eV, though the CCC results appear to do so closer to 100 eV. This, unfortunately, suggests that the "Born" limit, in the case of total ionisation, depends on the method of calculation. In the cross section peak region (10-20 eV) the Born-approximation calculations of Ton-That *et al* (1977) lie very close to the experiment data, and the Born-Ochkur calculations of Peach (Dixon *et al* 1976) lie substantially lower than experiment, indicating that the approximate inclusion of exchange in the calculation reduces the Born approximation cross section significantly in this region. Whereas at high energies auto- and double-ionisation process occur, which may account for the different "Born" limits, this is not the case in the region of 10 to 20 eV. Here only a single electron ejection is possible, and the frozen-core structure model should be sufficiently accurate.

Of particular significance to us is the remarkable agreement between the CCC theory and the measurements of the ionisation spin asymmetries A_i by Baum *et al* (1989). The A_i may be obtained from the doublet $\sigma_i^{(2)}$ and quartet $\sigma_i^{(4)}$ ionisation cross sections by

$$A_I = \frac{\sigma_i^{(2)} - \sigma_i^{(4)}}{\sigma_i^{(2)} + 2\sigma_i^{(4)}}. \tag{41}$$

The CCC(111) and CCC(75) calculations are very close indicating that convergence for spin asymmetry is somewhat easier to achieve than for total ionisation cross section. Note that the Born calculation of Ton-That *et al* (1977) would give exactly zero for the A_i. The ionisation asymmetry and cross section have a peak in the same energy region. Therefore agreement of the Born calculations with the experimental ionisation cross section in this region is likely to be accidental.

5.3. *Total cross sections*

Finally, we compare in figure 17 our results with measurements of the total cross sections for scattering on the $2^{1,3}$S states by Wilson and Williams (1976) and with the 5-state R-matrix calculations (Fon, Berrington, Burke and Kingston 1981). Experimental data are absolute for the 2^1S state and relative for the 2^3S state, which we have normalized to the CCC data at 7.94 eV. These are the least sensitive of the cross sections and are dominated by the elastic and optically-allowed transitions. Convergence is particular easy to achieve as can be seen from the the comparison of the 75-state CCC results with the 5-state R-matrix calculations. Good agreement with experiment exists for incident electron energies above approximately 1.5 eV. Below this energy the CCC results are substantially lower than experiment. This behavior of the CCC results is in agreement with the results of the 5-state R-matrix calculations, which are expected to be reliable for energies below the excitation thresholds of the $n = 3$ states.

6. Conclusions

We have presented a review of recent CCC calculations applied to the e-He system. Generally we find satisfactory agreement between theory and experiment for discrete transitions involving the ground state. Good agreement with experiment is also found for the case of differential ionisation with asymmetric energy sharing by the outgoing electrons. However, no such good agreement with experiment is found when scattering from the metastable 2^3S helium state is considered, even though these results are generated simultaneously with those for the ground state. Of particular concern is that the CCC results are systematically lower than a number of independent measurements. We suggest that further theoretical and experimental investigation of electron scattering on the metastable states of helium is warranted.

A very intriguing aspect of the CCC calculations that we have only been able to touch upon lightly is the application to the calculation of differential ionisation in the equal-energy-sharing kinematical region. While obtaining excellent angular profiles the theory underestimates the magnitudes. Investigation of the reasons for this is currently one of our highest priorities.

The CCC method has now been extended to general quasi-two-electron atoms and ions. Whereas for helium the frozen-core approximation has sufficed for our purposes this not so for other such targets. Furthermore, application to double ionisation and ionisation plus excitation by electron impact requires relaxation of the frozen-core approximation. We look forward to applying the CCC method to such processes.

Acknowledgments

We are indebted to Ian McCarthy and Andris Stelbovics for many useful discussions. We are grateful to Klaus Bartschat, David Cartwright, Albert Crowe, Morty Khakoo and Don Madison for communicating their data in electronic form The support of the Australian Research Council and The Flinders University of South Australia is gratefully appreciated. We also acknowledge the support of the South Australian Centre for High Performance Computing and Communications. Research sponsored in part by the Phillips Laboratory, Air Force Materiel Command, USAF, under cooperative agreement number F29601-93-2-0001.

References

Andersen N, Gallagher J W and Hertel I V 1988 *Phys. Rep.* **165**, 1–188
Bartschat K and Madison D H 1988 *J. Phys. B* **21**, 153–170
Bartschat K, Hudson E T, Scott M P, Burke P G and Burke V M 1996*a* *J. Phys. B* **29**, 2875–2885
Bartschat K, Hudson E T, Scott M P, Burke P G and Burke V M 1996*b* *J. Phys. B* **29**, 115–123
Baum G, Fink M, Raith W, Steidl H and Taborski J 1989 *Phys. Rev. A* **40**, 6734–6736
Beijers J P, Madison D H, van Eck J and Heideman H G M 1987 *J. Phys. B* **20**, 167–181
Berrington K A, Burke P G, Freitas L G and Kingston A E 1985 *J. Phys. B* **18**, 4135–4147
Berrington K A and Kingston A E 1987 *J. Phys. B* **20**, 6631–6640
Biswas R and Sinha C 1995 *Phys. Rev. A* **51**, 3766–3772
Blum K 1981 ***Density Matrix Theory and Applications*** Plenum Press New York
Brauner M, Briggs J S and Klar H 1991 *J. Phys. B* **24**, 287–297
Bray I 1994 *Phys. Rev. Lett.* **73**, 1088–1091
Bray I, Fursa D, Donnelly B P, McLaughlin D T and Crowe A 1995. In *AIP Conf. Proc. 360* Dubé L J, Mitchell J B A, McConkey J W and Brion C E, eds AIP Press, New York Whistler, Canada
Bray I and Fursa D V 1995 *J. Phys. B* **28**, L197–L202
Bray I and Fursa D V 1996*a* *Phys. Rev. A* **54**, 2991–3004
Bray I and Fursa D V 1996*b* *Phys. Rev. Lett.* **76**, 2674–2678
Bray I and Stelbovics A T 1992 *Phys. Rev. A* **46**, 6995–7011
Bray I and Stelbovics A T 1993 *Phys. Rev. Lett.* **70**, 746–749
Bray I, Konovalov D A, McCarthy I E and Stelbovics A T 1994 *Phys. Rev. A* 50, R2818–R2821
Bray I, McCarthy I E, Wigley J and Stelbovics A T 1993 *J. Phys. B* **26**, L831–836
Bray I, McCarthy I and Stelbovics A T 1996 *J. Phys. B* **49**, L245–L247
Briggs J S and Kim Y K 1971 *Phys. Rev. A* **3**, 1342–1349
Brunger M J, Buckman S J, Allen L J, McCarthy I E and Ratnavelu K 1992 *J. Phys. B* **25**, 1823–1838
Brunger M J, McCarthy I E, Ratnavelu K, Teubner P J O, Weigold A M, Zhou Y and Allen L J 1990 *J. Phys. B* **23**, 1325–1335
Byron F W and Joachain C J 1977 *Phys. Rev. A* **15**, 128–146
Byron F W, Joachain C J and Piraux B 1986 *J. Phys. B* **19**, 1201–1210
Cartwright D C, Csanak G, Trajmar S and Register D F 1992 *Phys. Rev. A* **45**, 1602–1623
Cartwright D C and Csanak G 1995 *Phys. Rev. A* **51**, 454–472

Chutjian A and Thomas L D 1975 *Phys. Rev. A* **11**, 1583–1595
Cohen M and McEachran R P 1967 *Proc. Phys. Soc.* **92**, 37–41
Crowe A, Donnelly B P, McLaughlin D T, Bray I and Fursa D V 1994 *J. Phys. B* **27**, L795–L801
Csanak G and Cartwright D C 1988 *Phys. Rev. A* **38**, 2740–2761
Curran E P and Walters H R J 1987 *J. Phys. B* **20**, 337–365
Curran E P, Whelan C T and Walters H R J 1991 *J. Phys. B* **24**, L19–L25
de Heer F J, Bray I, Fursa D V, Bliek F W, Folkerts H O, Hoekstra R and Summers H P 1995 *Atomic and Plasma-Material Interaction Data for Fusion* **6**, 7–26
Dewangan D P and Walters H R 1977 *J. Phys. B* **10**, 637–661
Dixon A J, Harrison M F A and Smith A C H 1976 *J. Phys. B* **9**, 2617–2631
Donnelly B P, McLaughlin D T and Crowe A 1994 *J. Phys. B* **27**, 319–328
Donnelly B P, Neill P A and Crowe A 1988 *J. Phys. B* **21**, L321–L325
Flannery M R and McCann K J 1975 *Phys. Rev. A* **12**, 846–855
Fon W C, Berrington K A, Burke P G and Kingston A E 1981 *J. Phys. B* **14**, 1041–1051
Fon W C, Berrington K A and Hibbert A 1981 *J. Phys. B* **14**, 307–321
Fon W C, Berrington K A and Kingston A E 1979 *J. Phys. B* **12**, 1861–1872
Fon W C, Berrington K A and Kingston A E 1991 *J. Phys. B* **24**, 2161–2182
Fon W C, Lim K P, Berrington K A and Lee T G 1995 *J. Phys. B* **28**, 1569–1583
Franz A and Altick P L 1992 *J. Phys. B* **25**, 1577–1590
Freitas L G, Berrington K A, Burke P G, Hibbert A, Kingston A E and Sinfailam A L 1984 *J. Phys. B* **17**, L303–L309
Fursa D V and Bray I 1995 *Phys. Rev. A* **52**, 1279–1298
Furtado F M and O'Mahony P F 1988 *J. Phys. B* **21**, 137–151
Hertel I V and Stoll W 1977 *Adv. Atom. Mol. Phys.* **13**, 113–228
Jacka M, Kelly J, Lohmann B and Buckman S J 1995 *J. Phys. B* **28**, L361–L366
Jones S, Madison D H, Franz A and Altick P L 1993 *Phys. Rev. A* **48**, R22–R25
Jung K, Müller-Fiedler R, Schlemmer P, Ehrhardt H and Klar H 1985 *J. Phys. B* **18**, 2955–2966
Khakoo M A, Roundy D and Rugamas F 1995 *Phys. Rev. Lett.* **75**, 41–44
Kim Y K and Inokuti M 1969 *Phys. Rev.* **181**, 205–214
Konovalov D A and McCarthy I E 1995 *J. Phys. B* **28**, L139–L145
LaBahn R W and Callaway J I 1970 *Phys. Rev. A* **2**, 366–369
Lagus M E, Boffard J B, Anderson L W and Lin C C 1996 *Phys. Rev. A* **53**, 1505–1518
Madison D H 1979 *J. Phys. B* **12**, 3399–3414
Mathur K C, McEachran R P, Parcell L A and Stauffer A D 1987 *J. Phys. B* **20**, 1599–1608
McAdams R, Hollywood M T, Crowe A and Williams J F 1980 *J. Phys. B* **13**, 3691–3701
McCarthy I E, Ratnavelu K and Zhou Y 1991 *J. Phys. B* **24**, 4431–4439
McGuire E J 1971 *Phys. Rev. A* **3**, 267–279
Mikosza A G, Hippler R, Wang J B and Williams J F 1993 *Phys. Rev. Lett.* **71**, 235–238
Mikosza A G, Hippler R, Wang J B and Williams J F 1996 *Phys. Rev. A* **53**, 3287–3294
Montague R G, Harrison M F A and Smith A C H 1984 *J. Phys. B* **17**, 3295–3310
Müller-Fiedler R, Jung K and Ehrhardt H 1986 *J. Phys. B* **19**, 1211–1229
Müller-Fiedler R, Schlemmer P, Jung K, Hotop H and Ehrhardt H 1984 *J. Phys. B* **17**, 259–268
Neill P A, Donnelly B P and Crowe A 1989 *J. Phys. B* **22**, 1417–1424
Neill P A and Crowe A 1988 *J. Phys. B* **21**, 1879–1886

Nesbet R K 1979 *Phys. Rev. A* **20**, 58–70
O'Malley T F, Burke P G and Berrington K A 1979 *J. Phys. B* **12**, 953–965
Rall D L, Sharpton F A, Schulman M B, Anderson L W, Lawler J E and Lin C C 1989 *Phys. Rev. Lett.* **62**, 2253–2256
Register D F, Trajmar S and Srivastava S K 1980 *Phys. Rev. A* **21**, 1134–1151
Röder J, Ehrhardt H, Bray I and Fursa D V 1996*a* *J. Phys. B* **29**, L421–L424
Röder J, Ehrhardt H, Bray I, Fursa D V and McCarthy I E 1996*b* *J. Phys. B* **29**, 2103–2114
Röder J, Ehrhardt H, Bray I, Fursa D V and McCarthy I E 1996*c* *J. Phys. B* **29**, L67–L73
Röder J, Ehrhardt H, Bray I and Fursa D V 1997*a* submitted to *J. Phys. B*
Röder J, Ehrhardt H, Bray I and Fursa D V 1997*b* submitted to *J. Phys. B*
Röder J, Jung K and Ehrhardt H 1995. private communication
Sawey P M J, Berrington K A, Burke P G and Kingston A E 1990 *J. Phys. B* **23**, 4321–4329
Scott T and Taylor H S 1979 *J. Phys. B* **12**, 3385–3397
Stelbovics A T 1990 *Phys. Rev. A* **41**, 2536–2545
Steph N C and Golden D E 1983 *Phys. Rev. A* **27**, 1678–1681
Ton-That D, Manson S T and Flannery M R 1977 *J. Phys. B* **4**, 621–635
Trajmar S, Register D F, Cartwright D C and Csanak G 1992 *J. Phys. B* **25**, 4889–4910
van den Heuvell H B V L, van Eck J and Heideman H G M 1982 *J. Phys. B* **15**, 3517–3533
Verma S, Srivastava R and Itikawa Y 1995 *J. Phys. B* **28**, 1023–1048
Weiss A W 1967 *J. Res. Natl. Bur. Stand. A* **71**, 163–
Wilson W G and Williams W L 1976 *J. Phys. B* **9**, 423–432
Winters K H, Clark C D, Bransden B H and Coleman J P 1974 *J. Phys. B* **4**, 146–154
Younger S M 1981 *J. Quant. Spectrosc. Radiat. Transfer* **26**, 329–337

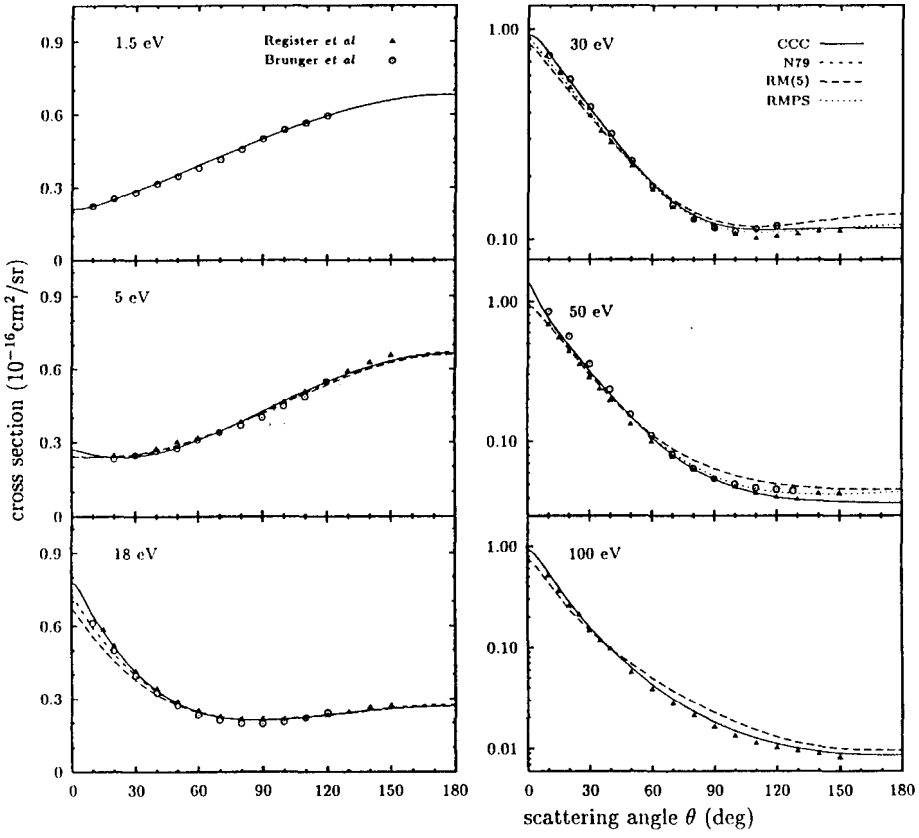

Figure 1. Elastic differential cross sections for e-He scattering at a range of projectile energies. The measurements are due to Brunger *et al* (1992) and Register *et al* (1980). The CCC calculations are due to Fursa and Bray (1995), except at 30 eV where they are due to the present 111-state calculation. The R-matrix with pseudostates (RMPS) calculations at 30 and 50 eV are due to Bartschat *et al* (1996*a*). The variational calculations of Nesbet (1979) at 5 and 18 eV are denoted by N79, and the 5-state R-matrix calculations of Fon, Berrington and Hibbert (1981) are denoted by RM(5).

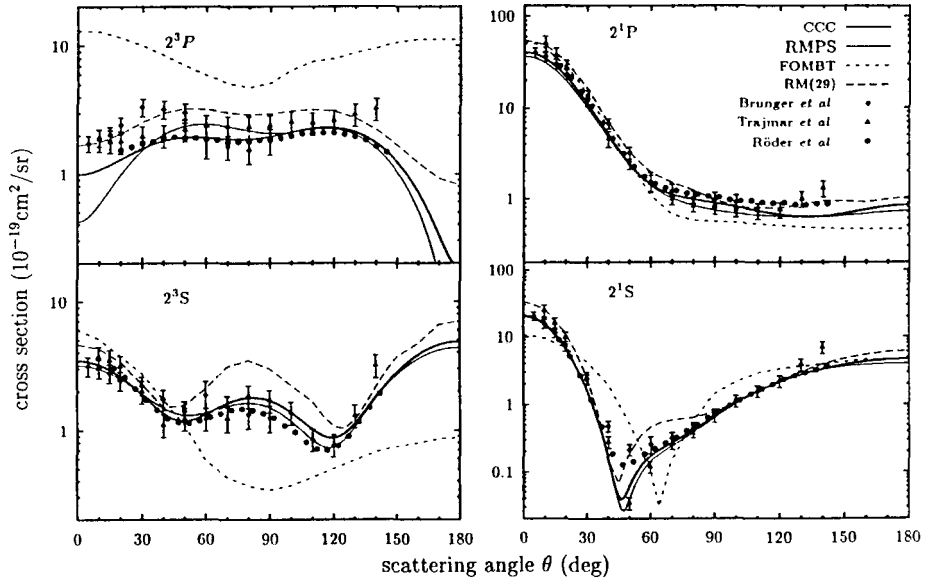

Figure 2. The $2^{1,3}$S and $2^{1,3}$P differential cross sections for e-He scattering at 30 eV. The measurements are due to Brunger *et al* (1990), Trajmar *et al* (1992), and Röder *et al* (1996*a*) (normalized to CCC). The present 111-state CCC calculation is described in the text. The recent R-matrix with pseudostates (RMPS) results are due to Bartschat *et al* (1996*a*). The calculations denoted by RM(29) are due to Fon *et al* (1995), and those denoted by FOMBT are due to Cartwright *et al* (1992).

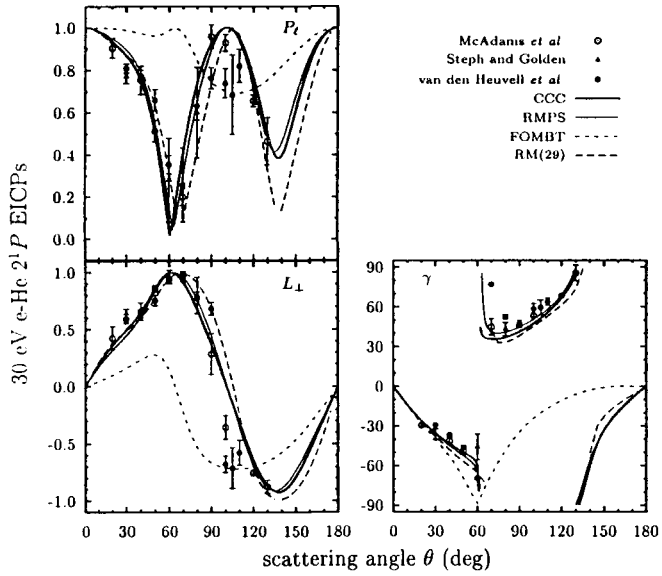

Figure 3. The 2^1P EICP's for e-He scattering at 30 eV. The present CCC calculation is described in the text. The RMPS results are due to Bartschat *et al* (1996*a*). The calculations denoted by RM(29) are due to Fon *et al* (1995), and those denoted by FOMBT are due to Cartwright *et al* (1992). The measurements are due to McAdams *et al* (1980), Steph and Golden (1983), and van den Heuvell *et al* (1982).

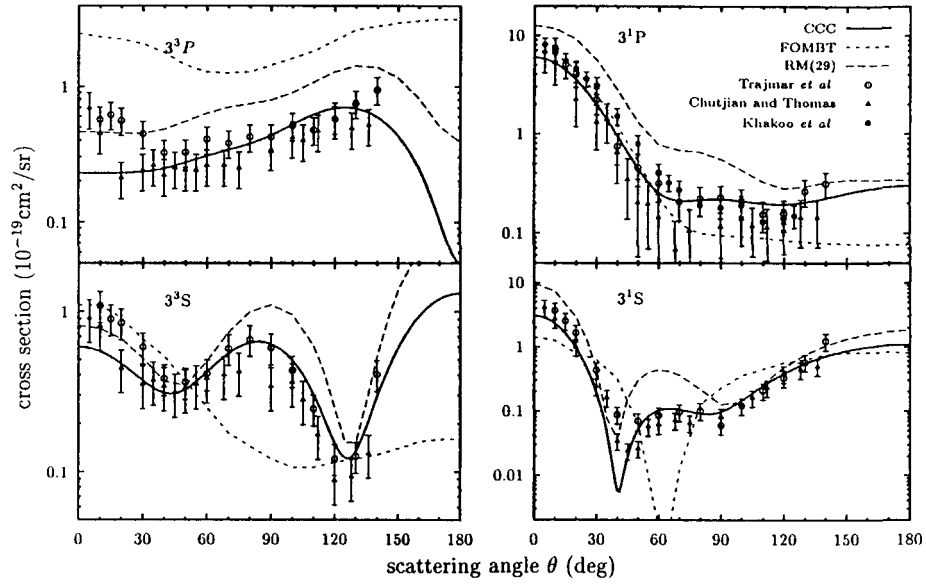

Figure 4. The $3^{1,3}$S and $3^{1,3}$P excitation differential cross sections for e-He scattering at 30 eV. The present CCC calculation is described in the text. The calculations denoted by RM(29) are due to Fon *et al* (1995), and those denoted by FOMBT are due to Cartwright *et al* (1992). The measurements due to Chutjian and Thomas (1975) and Trajmar *et al* (1992) are of the summed 3^1P $+3^{3,1}$D cross sections, and have had the CCC results for the $3^{3,1}$D states subtracted. The data of Khakoo *et al* (1995) is solely for the 3^1P excitation, obtained with the aid of the electron-photon coincidence technique.

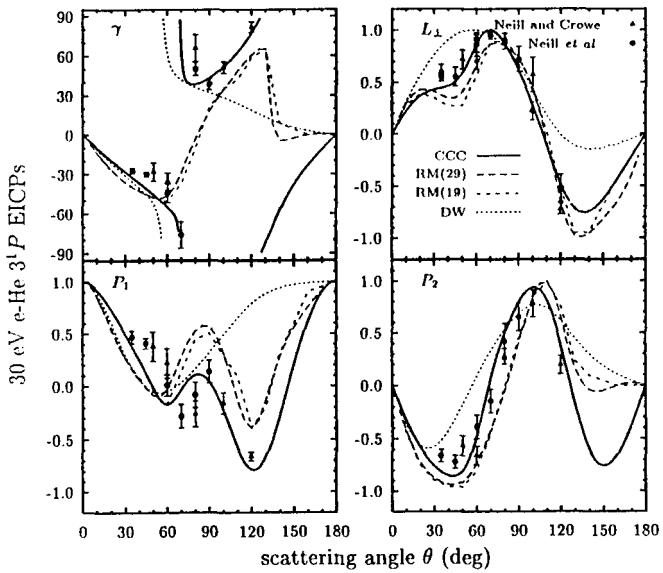

Figure 5. The 3^1P EICPs for e-He scattering at 30 eV. The present CCC calculation is described in the text. The calculations denoted by RM(19) and RM(29) are due to Fon *et al* (1991) and Fon *et al* (1995), respectively. The calculations denoted by DW are due to Beijers *et al* (1987). The measurements are due to Neill and Crowe (1988) and Neill *et al* (1989).

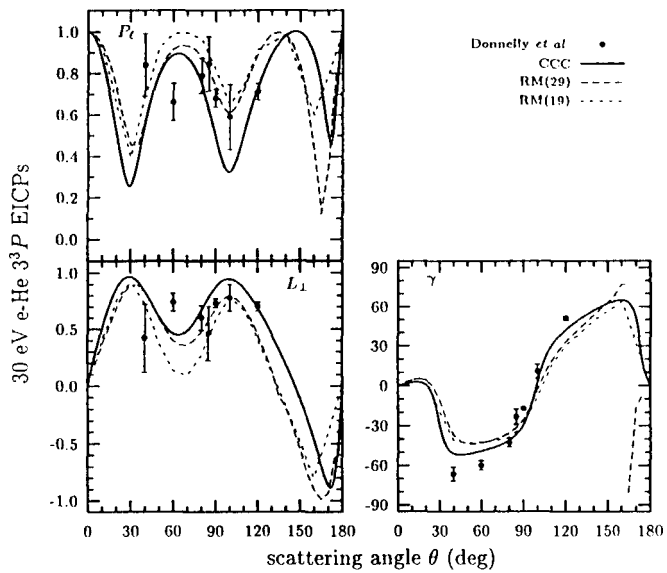

Figure 6. The 3^3P EICPs for e-He scattering at 30 eV. The present CCC calculation is described in the text. The calculations denoted by RM(19) are due to Fon *et al* (1991), RM(29) are due to Fon *et al* (1995). The measurements are due to Donnelly *et al* (1988).

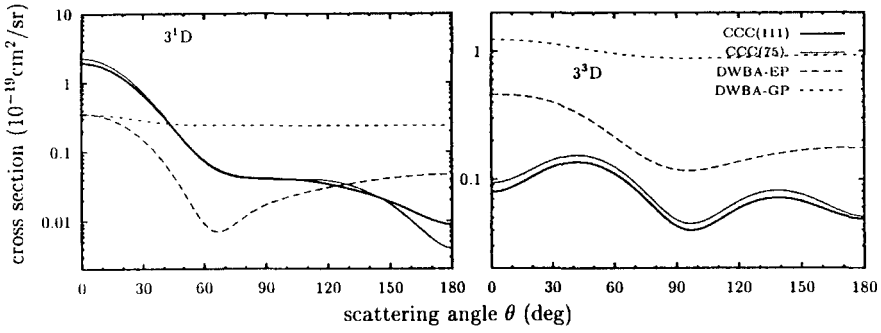

Figure 7. The $3^{1,3}$D excitation differential cross sections for e-He scattering at 30 eV. The present CCC(111) calculation is described in the text. The CCC(75) calculation (Fursa and Bray 1995) is given to show convergence in the CCC approach by contrast to the dependence of the cross sections upon the choice of distortion in the DW calculations of Bartschat and Madison (1988).

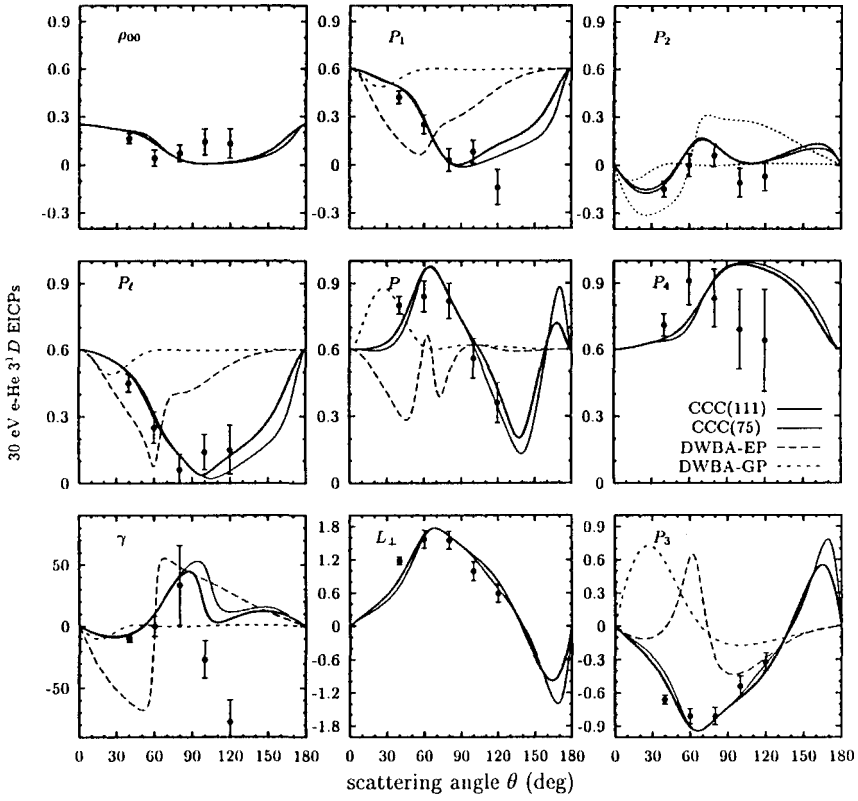

Figure 8. The 3^1D EICPs for 30 eV e-He scattering. The present 111-state convergent close-coupling calculation is denoted by CCC(111). The CCC(75) calculation is due to (Fursa and Bray 1995). The calculations denoted by DWBA-EP and DWBA-GP are due to Beijers *et al* (1987). The measurements are due to Donnelly *et al* (1994).

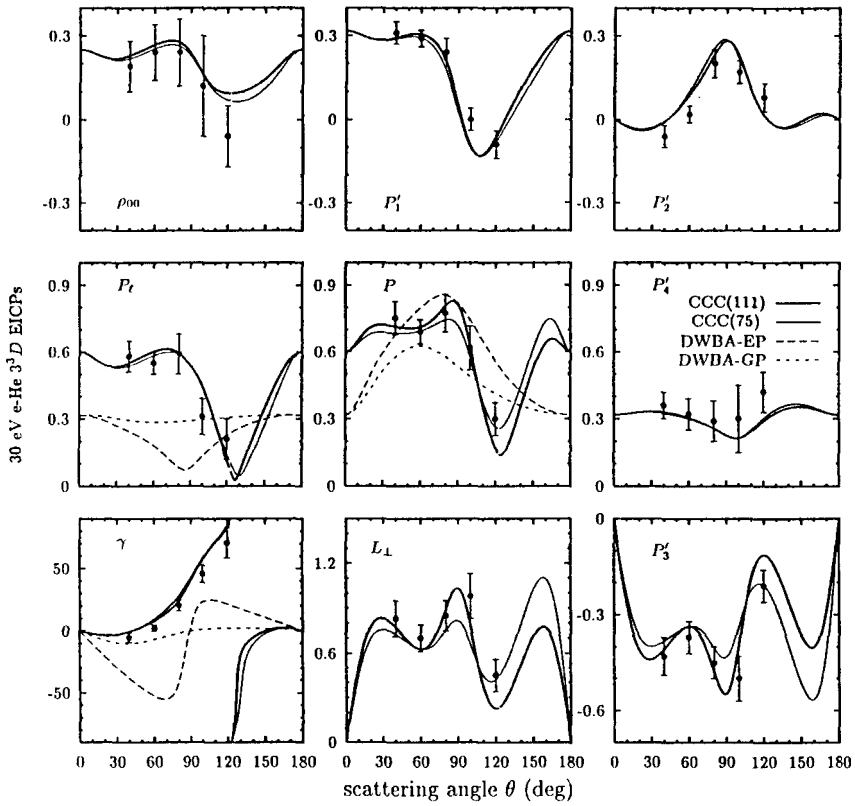

Figure 9. The 3^3D EICPs and observed Stokes parameters for 30 eV e-He scattering. The theory is same as in figure 8. The preliminary measurements have been reported by Bray *et al* (1995).

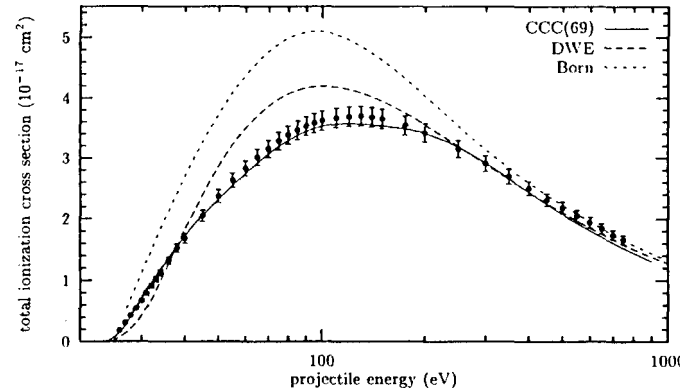

Figure 10. Total ionisation cross sections of the 1^1S state of helium by electron impact. The convergent close-coupling calculations are denoted by CCC(69). The Born and distorted wave with exchange (DWE) calculations are due to McGuire (1971) and Younger (1981), respectively. The measurements are due to Montague *et al* (1984).

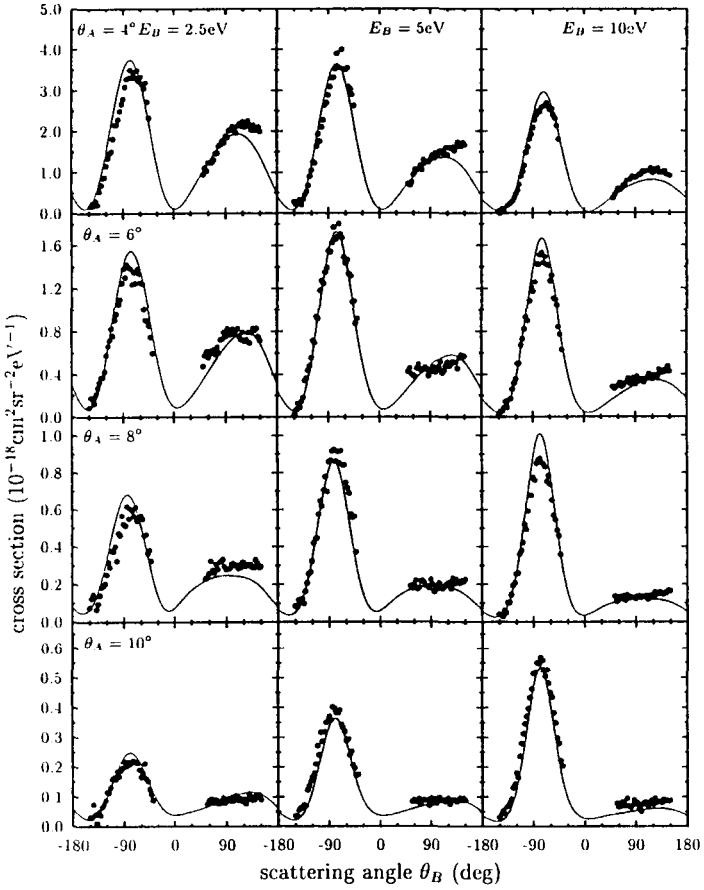

Figure 11. Electron-impact ionisation of helium triple differential cross sections at 600 eV. The CCC(51) calculation is due to Bray and Fursa (1996*a*). The measurements are due to Jung *et al* (1985).

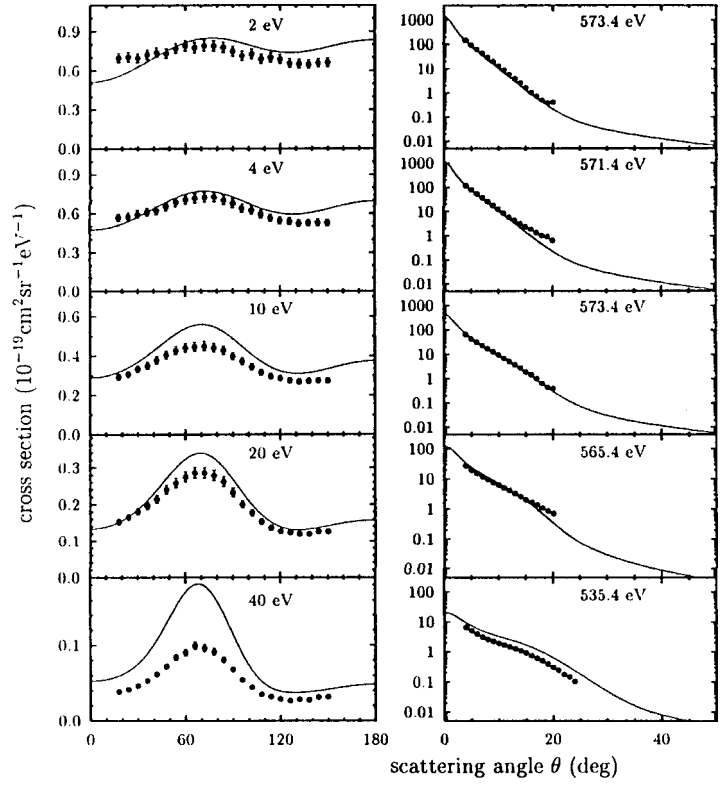

Figure 12. Electron-impact ionisation of helium double differential cross sections at 600 eV. The CCC(51) calculation is due to Bray and Fursa (1996*a*). The measurements are due to Müller-Fiedler *et al* (1986).

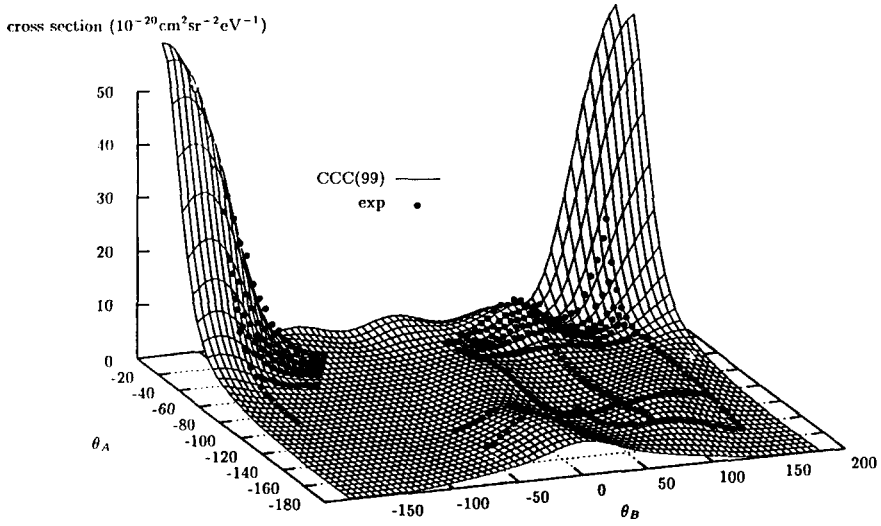

Figure 13. The e-He ionisation coplanar triple differential cross sections for the case of 40 eV incident energy with the slow $E_B = 4$ eV electron detected at θ_B and the fast $E_A = 11.4$ eV electron detected at θ_A. The absolute measurements and the 99-state CCC calculation are from Röder *et al* (1996*b*).

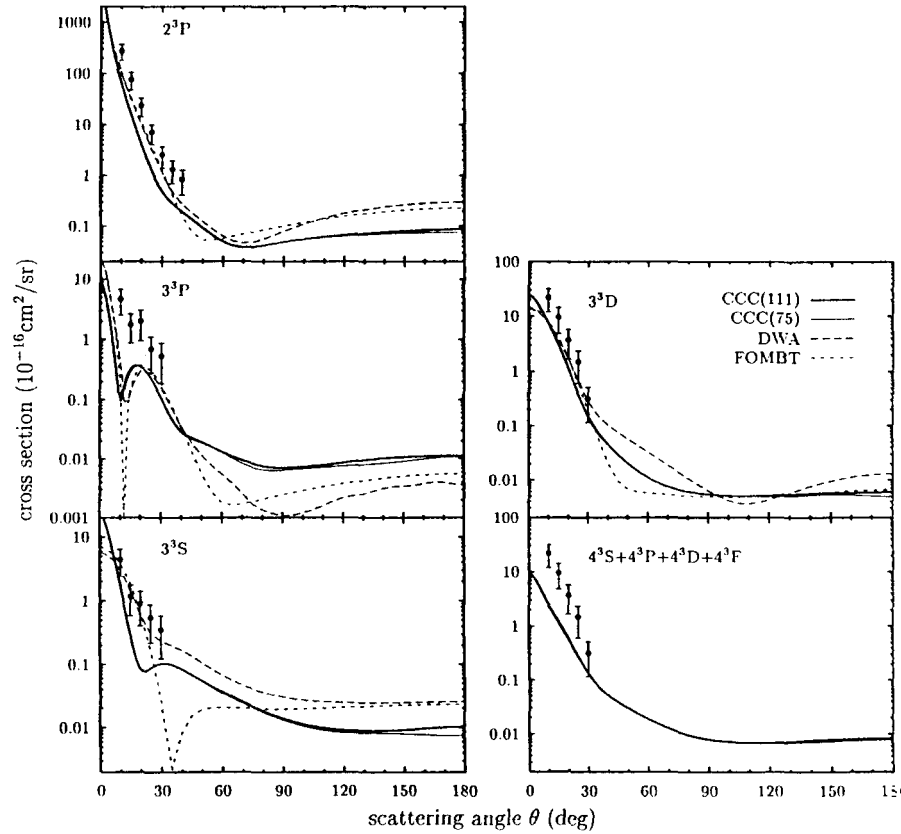

Figure 14. Differential cross sections for excitation of the helium 2^3S state. The CCC(75) (Bray and Fursa 1995) and present CCC(111) calculations are for 21 eV incident electrons, leading to outgoing energies of approximately 20 eV. The measurements at outgoing energy of 20 eV are due to Müller-Fiedler *et al* (1984). The DWA and the FOMBT results are due to Cartwright and Csanak (1995).

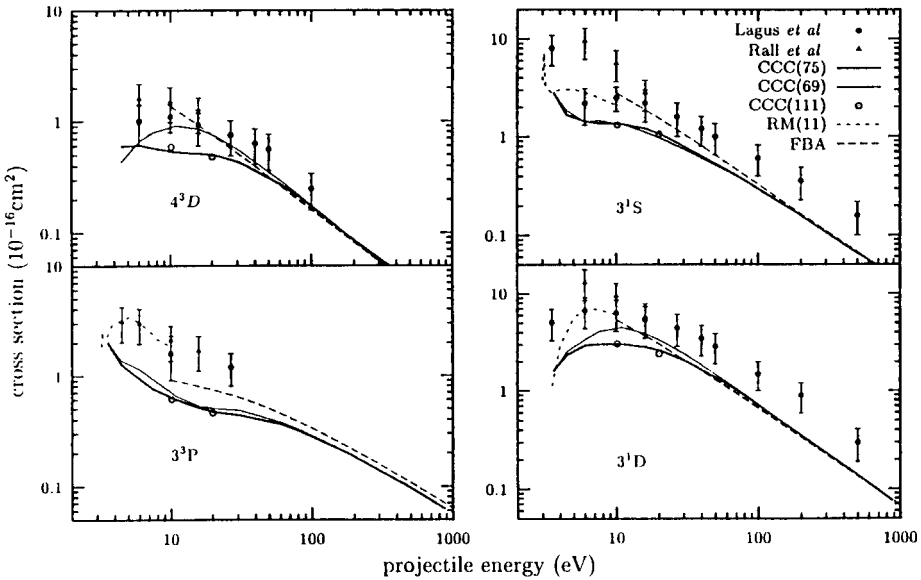

Figure 15. Integrated cross sections for scattering from metastable 2^3S helium state. The present 111-state calculations are denoted by CCC(111). The CCC(75) and CCC(69) calculations are from de Heer *et al* (1995) The Born (FBA) calculations are due to Briggs and Kim (1971) and 11-state R-matrix calculations RM(11) are due to Berrington *et al* (1985). The measurements are due to Rall *et al* (1989) and Lagus *et al* (1996).

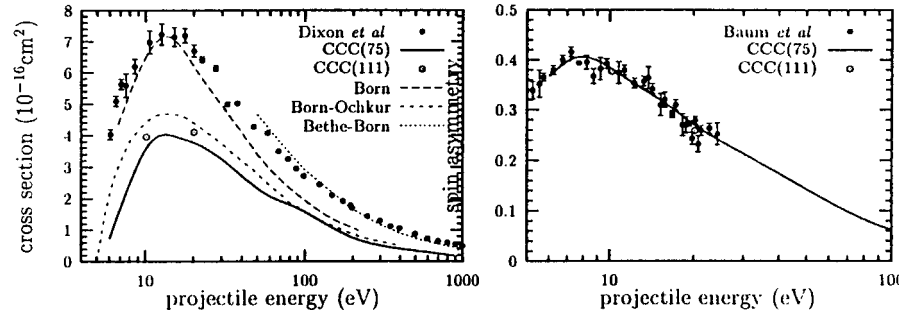

Figure 16. Total ionisation cross section and its spin asymmetry for electron impact ionisation of the 2^3S state of helium. The present 111-state calculations are denoted by CCC(111), the CCC(75) is due to (Bray and Fursa 1995). The Born, Born-Ochkur and Bethe-Born calculations are due to Ton-That *et al* (1977), Peach (Dixon *et al* 1976) and Briggs and Kim (1971), respectively. The measurements are due to Dixon *et al* (1976) and Baum *et al* (1989).

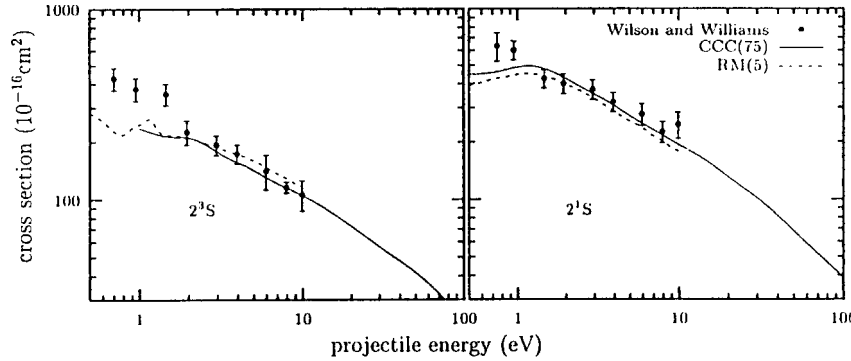

Figure 17. Total cross sections for electron scattering from the 2^3S and 2^1S states of helium. The convergent close-coupling calculations are denoted by CCC(75) (Bray and Fursa 1995). The calculations denoted by RM(5) are due to Fon, Berrington, Burke and Kingston (1981). The measurements are due to Wilson and Williams (1976). For 2^1S state measurements are absolute, while for 2^3S state they are relative and are normalized to the CCC data (1.158×10^{-14} cm^2) at 7.94 eV.